Human Acyl-Coenzyme A:Cholesterol Acyltransferase Expressed in Chinese Hamster Ovary Cells: Membrane Topology and Active Site Location

Song Lin, Xiaohui Lu, Catherine C.Y. Chang, and Ta-Yuan Chang[†]

Department of Biochemistry, Dartmouth Medical School, Hanover, New Hampshire 03755

Acyl-CoA:cholesterol acyltransferase (ACAT) is a membrane-bound enzyme that produces cholesteryl esters intracellularly. Two ACAT genes (*ACAT1* and *ACAT2*) have been identified. The expression of ACAT1 is ubiquitous, whereas that of ACAT2 is tissue restricted. Previous research indicates that ACAT1 may contain seven transmembrane domains (TMDs). To study ACAT2 topology, we inserted two different antigenic tags (hemagglutinin, monoclonal antibody Mab1) at various hydrophilic regions flanking each of its predicted TMDs, and expressed the recombinant proteins in mutant Chinese hamster ovary cells lacking endogenous ACAT. Each tagged ACAT2 was expressed in the endoplasmic reticulum as a single undegraded protein band and was at least partially active enzymatically. We then used cytoimmunofluorescence and protease protection assays to monitor the sidedness of the hemagglutinin and Mab1 tags along the ER membranes. The results indicated that ACAT2 contains only two detectable TMDs, located near the N terminal region. We also show that a conserved serine (S245), a candidate active site residue, is not essential for ACAT catalysis. Instead, a conserved histidine (H434) present within a hydrophobic peptide segment, may be essential for ACAT catalysis. H434 may be located at the cytoplasmic side of the membrane.

INTRODUCTION

Acyl CoA:cholesterol acyltransferase (ACAT) is an intracellular enzyme that uses cholesterol and long-chain fatty acyl CoA as substrates to produce cholesteryl esters (Chang *et al.*, 1997). In mammals, two ACAT genes, *ACAT1* and *ACAT2*, have been discovered (Chang *et al.*, 1993; Anderson *et al.*, 1998; Cases *et al.*, 1998a; Oelkers *et al.*, 1998; Buhman *et al.*, 2000a; Rudel *et al.*, 2001; Chang *et al.*, 2001a; Buhman *et al.*, 2001). The proteins encoded by *ACAT1* and *ACAT2* share extensive homology near their C termini but not near their N termini. Specific antibodies against the N-terminal segments of human ACAT1 (hACAT1) (Chang *et al.*, 1995) or human ACAT2 (hACAT2) (Chang *et al.*, 2000) were used to study the tissue distribution of these two isoenzymes. In adult human tissues, ACAT1 is found in almost all of the cell types and tissues

examined (Lee *et al.*, 1998; Chang *et al.*, 2000; Sakashita *et al.*, 2000). In contrast, ACAT2 protein is mainly found in the apical region of the intestinal villi. Low levels of hACAT2 can also be found in adult human hepatocytes (Chang *et al.*, 2000) and in activated macrophages (our unpublished data). In mice and monkeys, the relative tissue distributions of ACAT1 and ACAT2 are similar but not identical to those found in humans (Meiner *et al.*, 1997; Buhman *et al.*, 2000b; Lee *et al.*, 2000). Based on studies in tissue distribution and genetic studies in mice (Meiner *et al.*, 1996; Buhman *et al.*, 2000b; Spady *et al.*, 2000; Yagyu *et al.*, 2000), ACAT1 may play a critical role in macrophage foam-cell formation, whereas ACAT2 may play a critical role in the cholesterol absorption process. The exact physiological roles of ACAT1 and ACAT2 in various cell types are under active investigation.

The enzymological properties of hACAT1 and hACAT2 are very similar (Chang *et al.*, 2000). ACAT1 is a homotetrameric enzyme (Yu *et al.*, 1999, 2002) and is mainly located in the endoplasmic reticulum (ER) (Chang *et al.*, 1995; Sakashita *et al.*, 2000). The subunit composition and the precise location of ACAT2 are unknown at present. Sparse information is available regarding the ACAT active site(s): a conserved serine residue present in ACAT1 (S269), ACAT2 (S245), and the enzyme diacylglycerol acyltransferase 1 (Cases *et al.*, 1998b; Buhman *et al.*, 2001) may be part of the active site (Cao *et al.*, 1996; Joyce *et al.*, 2000). On the other

hand, a superfamily of membrane-bound *O*-acyltransferases has been identified (Hofmann, 2000). A histidine (460 in hACAT1 and 434 in hACAT2) within a long hydrophobic region is invariant within this family, suggesting that it may be part of the active site. The suggestions that the conserved serine and/or the conserved histidine may constitute part of the ACAT active site were based on computer analysis, not based on experimental data. Several residues may be involved in binding between ACAT and its substrates (Guo *et al.*, 2001). Cysteines are not needed for ACAT1 catalysis (Lu *et al.*, 2002b).

Both ACAT1 and ACAT2 may contain multiple transmembrane domains (TMDs). Previously, we created various hACAT1 constructs tagged at various hydrophilic regions with a nine amino acid (a.a.) antigenic tag (hemagglutinin epitope tag, HA) and then expressed the tagged constructs in mutant Chinese hamster ovary (CHO) cells lacking endogenous ACAT1 (AC29) (Cadigan *et al.*, 1988; Chang *et al.*, 1993). Indirect immunofluorescence microscopy was used to determine the topology of the tagged proteins. The results showed that ACAT1 contains at least seven TMDs (Lin *et al.*, 1999). In the current study, we used the same strategy, as well as a protease protection assay to study the hACAT2 topology. The results using different approaches corroborated one another, enabling us to produce a membrane topology model for ACAT2. We also performed site-specific mutagenesis experiments and identified the putative active site of ACAT. Joyce and colleagues had reported previously that both ACAT1 and ACAT2 (from monkey) contained five TMDs (Joyce *et al.*, 2000). The same investigators also proposed that a conserved serine residue (S245 in human ACAT2) might comprise part of the ACAT active site. Their results are very different from ours. In the DISCUSSION, we suggested several clues that might explain the difference in results seen between our work and the work of Joyce and colleagues.

MATERIALS AND METHODS

Reagents

Goat anti-rabbit IgG conjugated with Alexa 594 and goat anti-mouse IgG conjugated with Alexa 488 were from Molecular Probes (Eugene, OR). Trypsin was from Promega (Madison, WI). Soybean trypsin inhibitor was from Sigma-Aldrich. The anti-ACAT1 monoclonal antibody (mAb) Mab1 was from Vancouver Biotech (Vancouver, BC, Canada). The high-titer polyclonal antibodies against the N-terminal peptide region of hACAT2 (DM54 and DM56) were described previously (Chang *et al.*, 2000). DM94 are rabbit polyclonal antibodies against ACAT2 peptide$_{a.a.\ 384-433}$. They were produced by using the glutathione *S*-transferase (GST) fusion protein technology described previously (Chang *et al.*, 1995). As the antigen, the GST was fused at the N terminus of a peptide comprised of two repeats of the ACAT2 peptide$_{a.a.\ 384-433}$. The DM94 antiserum was affinity purified using the GST-ACAT2 peptide$_{a.a.\ 384-433}$ affinity column, according to procedure described previously (Chang *et al.*, 1995). The sources of all other reagents were the same as described previously (Lin *et al.*, 1999).

Methods

The Construct HisACAT2.
The *HisACAT2* construct was created previously (Chang *et al.*, 2000) and contains the HisT7 tag at the N terminus of hACAT2. The HisT7 tag has 34 amino acids, including

a six-histidine tag, a T7 tag with 11 amino acids, and an enterokinase cleavage recognition sequence (Invitrogen, Carlsbad, CA).

The ACAT2 Constructs Containing the Hemagglutinin (HA) Tag.
The hemagglutinin epitope tag (HA tag) (Kolodziej and Young, 1991) was inserted into the ACAT2 protein at each of the 10 specific sites as indicated in Figure 2, A and C.; the specific amino acid after which the HA tag was inserted has been indicated in the parentheses of Figure 2C. The various *ACAT2-HA* constructs were constructed by a general procedure that involved ligating two specific polymerase chain reaction (PCR) fragments of *hACAT2* cDNA. The design of the PCR primers took advantage of the fact that the protein coding sequence of *hACAT2* cDNA did not contain any EcoR1 sites. The first primer set was designed to produce a PCR fragment from the N terminus to the specific insertion site. The 5′ primer contained the *Hind*III sequence followed by the ACAT2 N-terminal–specific sequence; the 3′ primer contained the ACAT2 sequence before the insertion site, followed by the HA sequence and the EcoR1 sequence (GAATTC, which encodes the two amino acids glutamine and phenylalanine). The second primer set was designed to produce a PCR fragment from the ACAT2 sequence after the insertion site to the ACAT2 C termini, with an EcoR1 site at the 5′ end and a T7 tag sequence and an *Xba*I sequence at the 3′ end. The 5′ primer contained the EcoR1 site followed by the ACAT2 sequence after the insertion site; the 3′ primer contained the ACAT2 C-terminal sequence followed by a T7 tag sequence and an *Xba*I sequence. The two resultant PCR fragments were ligated into the expression vector p*cDNA3* between its unique *Hind*III and *Xba*I sites. This procedure resulted in the insertions of the nine amino acid-HA peptide sequences followed by the two amino acids glutamine and phenylalanine at each indicated site. The identities of the various p*cDNA3-ACAT2-HA* constructs were all confirmed by DNA sequencing.

The ACAT2 Constructs Containing Mab1 Tag.
The Mab1 tag, recognized by the ACAT1 mAb Mab1, is the first 64 amino acids of hACAT1 (Chang *et al.*, 1993). To produce various *ACAT2* constructs containing the Mab1 tag, two PCR primers were used to generate a Mab1 fragment with an EcoR1 site at both ends, by using the *hACAT1* cDNA coding region (Chang *et al.*, 1993) as a template. Then the Mab1 fragment was inserted into the unique EcoR1 site present in each of the *ACAT2-HA* constructs described above. This procedure inserted the Mab1 sequence flanked by the two amino acids glutamine and phenylalanine at each side. The orientation of the inserted Mab1 fragment was first diagnosed by PCR and then confirmed by DNA sequencing; those with the correct orientations were selected for further studies.

The ACAT2 Constructs Containing Various Single Substitution Mutations.
Various ACAT2 point mutants were generated by high-fidelity PCR-based mutagenesis, using Stratagene's QuikChange site-directed mutagenesis kit, according to procedures described previously (Lu *et al.*, 2002b). The identities of the various point mutations produced were all confirmed by DNA sequencing.

Procedures for Trypsin Protection Assay.
Two methods were used. Method 1 used microsomal vesicles. AC29 cells were grown in medium A in 25-cm² flasks to ~75% confluence. For each flask, 3 μg of individual recombinant *ACAT2 cDNA* as indicated, and 6 μl of LipofectAMINE were used to transfect the cells according to the company's manual. On the 2nd day after transfection, cells were rinsed twice with phosphate-buffered saline (PBS) and once with buffer B at 4°C (10 mM HEPES, pH 7.4, 10 mM KCl, 1.5 mM MgCl$_2$, 100 mM NaCl) and were collected by scraping and centrifugation at 4°C. All subsequent operations were kept at 4°C unless stated otherwise. The cells were homogenized for 20 strokes with a handheld stainless-steel tissue grinder (Dura-Grind; Wheaton, Millville, NJ). Microscopic examinations assured that the cell breakage was 99% complete. The whole cell lysates were transferred into 1.5-ml

Eppendorf tubes. Each tube contained 50 μg of protein. Triton X-100 was added to samples 6 to 10 (at 1% final concentration), but not to samples 1 to 5. Samples were finger-tapped, incubated for 1 min, and then a certain amount of trypsin as indicated was added. Trypsin was prepared as 239 U/ml stock solution in 10 mM HCl, and stored at −20°C; serial dilutions were freshly made from the stock and served as working solutions for each experiment. The samples were incubated at room temperature for 15 min. Adding 2 μl/sample of soybean trypsin inhibitor stock solution (at 100 μg/μl) inactivated the trypsin digestion. Ten microliters of 5× loading buffer was added per sample for SDS-PAGE. Method 2 used permeabilized cells grown in monolayer. The method was based on the procedure described by Macri and Adeli, (1997) with minor modifications. AC29 cells were grown in medium A in 12-well plates to ~80% confluence. To each well, 0.5 μg of individual Mab1-tagged *ACAT2* cDNAs and 6 μl of FuGene 6 (Roche Diagnostics, Indianapolis, IN) were used to transfect the cells according to the company's manual. Twenty-four hours after transfection, cells were rinsed with PBS with 10 mM dithiothreitol (DTT) and then permeabilized with either digitonin (0.002%) in buffer D (0.3 M sucrose, 0.1 M KCl, 2.5 mM MgCl$_2$, 20 mM 1,4-piperazinediethanesulfonic acid, 10 mM DTT, pH 6.8) or with saponin (0.025%) in PBS with 10 mM DTT, 1.0 ml/well, at room temperature for 10 min. Afterwards, 0.5 ml of buffer D with 10 mM DTT was added to each well. Adding various amount of trypsin (as indicated in the figure legend) started the protease digestions. The digestions proceeded at room temperature for 10 min and were stopped by adding 100 μg of trypsin inhibitor per well. The samples were solubilized with 8 M urea, 0.1 M DTT at 75 μl/well. Twenty-five microliters of 5× SDS loading buffer per well was added, and the samples were analyzed by SDS-PAGE.

Other procedures, including cells and transient transfection experiments, immunoblot analysis, ACAT activity assay in intact cells, and cytoimmunofluorescence assays have all been described in our previous work reporting the membrane topology of recombinant human ACAT1 expressed in AC29 cells (Lin *et al.*, 1999).

RESULTS

Selective Permeabilization of CHO Cells with Digitonin or Saponin

Our approach is to express various recombinant ACAT2 in AC29 cells. We then treat the cells with digitonin (an impure form of the detergent saponin) at low concentration to permeabilize the plasma membrane, or with saponin at high concentration to permeabilize the plasma membrane and the internal membranes. These treatments allow selective access of antibodies to the cell cytoplasm only, or to the cell cytoplasm and the lumen of the internal membranes. We then use the method of cytoimmunofluorescence to monitor the location of the tag inserted at various sites within ACAT2. To validate the selective membrane permeabilization procedure, we treated AC29 cells with digitonin at low concentration (0.0005%), and performed double cytoimmunofluorescence experiments. The use of double immunofluorescence ensured that the investigators were viewing two different targets from the same group of cells. We chose appropriate filters such that the anti-tubulin antibodies were seen in green and the anti-BiP antibodies were seen in red. The results showed that tubulin, a cytoplasmic protein marker, was fully visible, whereas BiP, the lumenal ER protein marker (Otto and Smith, 1994), was not visible (Figure 1, top, the first two frames from the left). When we treated the cells with saponin at high concentration (0.25%), both tubulin and BiP became fully visible (Figure 1, top, third and fourth frames from the left). BiP remained within
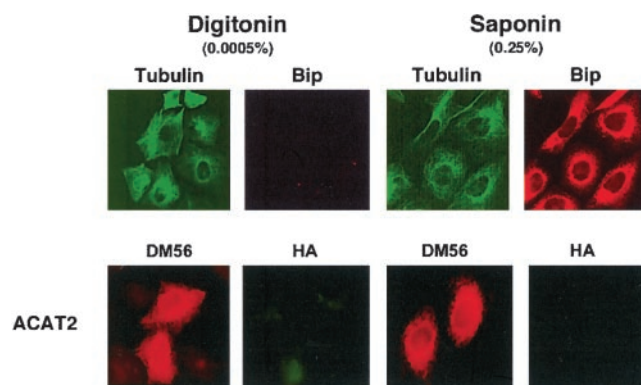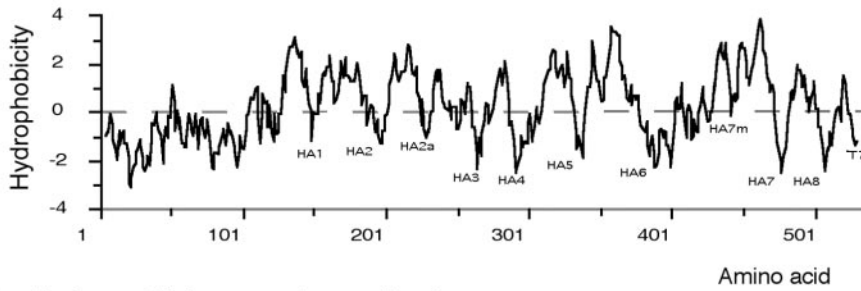

Figure 1. Permeabilization of AC29 cells with digitonin at 0.0005% or with saponin at 0.25%. Cells grown on glass coverslips were fixed with paraformaldehyde then permeabilized with either digitonin or with saponin as indicated. The double immunostainings were performed according to methods described in the MATERIALS AND METHODS. First row, AC29 cells were used; anti-tubulin (viewed in green) and anti-BiP (viewed in red) were used as the primary antibodies. Second row, AC29 Cells transiently transfected with *hACAT2* cDNA were used; DM56 (antibodies against the N-terminal segment of hACAT2; viewed in red) and anti-HA antibodies (viewed in green) were used as the primary antibodies.

the ER lumen and displayed a reticular pattern, because the cells were fixed with paraformaldehyde before they were permeabilized and stained with the anti-BiP antibodies. We next transfected AC29 cells with the untagged ACAT2 construct, and performed double immunofluorescence staining again. We used the high titer polyclonal antibodies (DM56) against the N-terminal peptide region of hACAT2 (Chang *et al.*, 2000), and the antibodies against the HA tag as the two primary antibodies. The DM56 antibodies were seen in red, and the anti-HA antibodies were seen in green. The results show that the N-terminal segment of ACAT2 was fully visible in both digitonin-treated cells and in saponin-treated cells (Figure 1, bottom, first and the third frames from the left). Higher magnification of these same cells indicated that the staining pattern was mainly confined at the nuclear envelope and at the reticulate network. In addition, double immunostaining experiments using anti-ACAT2 antibodies and anti-BiP antibodies showed extensive colocalization of the two signals, indicating that ACAT2 is mainly located in the ER membranes (our unpublished data). Because the ACAT2 construct used was untagged, the stainings using anti-HA antibodies resulted in no signal in either digitonin-treated or saponin-treated cells (Figure 1, bottom, second and fourth frames from the left).
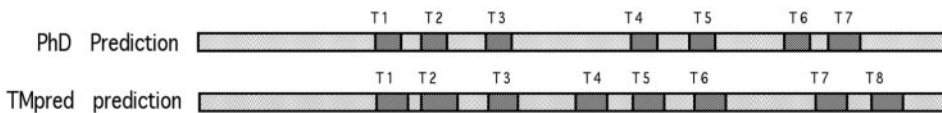
Cytoimmunofluorescence of Various T7-tagged or HA-tagged ACAT2

Based on the Kyte and Doolittle plot, ACAT2 is a hydrophobic protein with multiple TMDs (Figure 2A). It would be ideal to probe the sidedness of various hydrophilic regions flanking each putative TMD, by using specific antibodies that recognize each of these regions. However, after repeated attempts, we were only able to produce antibodies against the N-terminal (DM56 or DM54) and antibodies
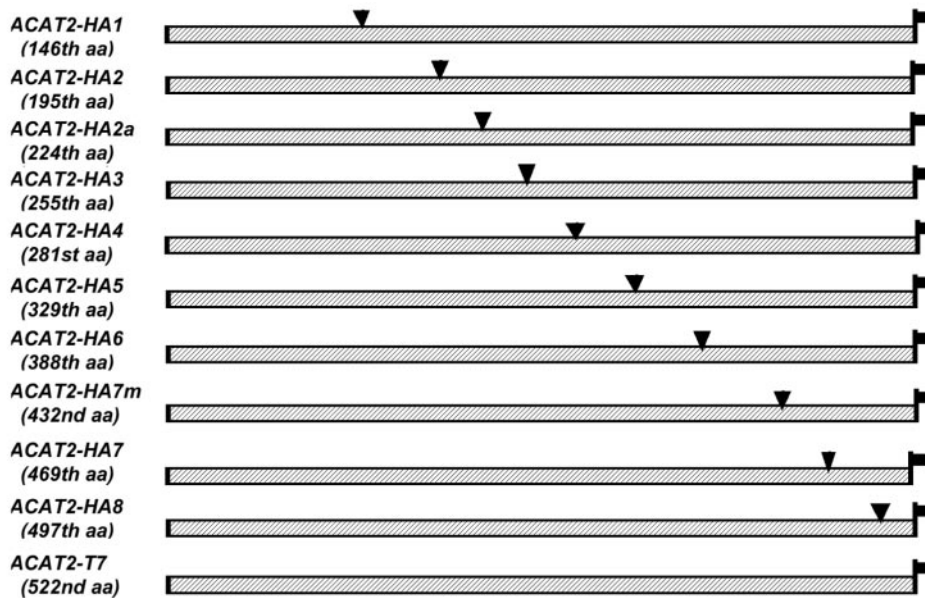
A. Hydropathy of ACAT2 Protein (Kyte & Doolittle):

B. Predictions of Transmembrane Regions:

C. Epitope-Tagged ACAT2 Constructs:

ACAT2-HA1 (146th aa)
ACAT2-HA2 (195th aa)
ACAT2-HA2a (224th aa)
ACAT2-HA3 (255th aa)
ACAT2-HA4 (281st aa)
ACAT2-HA5 (329th aa)
ACAT2-HA6 (388th aa)
ACAT2-HA7m (432nd aa)
ACAT2-HA7 (469th aa)
ACAT2-HA8 (497th aa)
ACAT2-T7 (522nd aa)

▼ HA tag (9 a.a.): Tyr-Pro-Tyr-Asp-Val-Pro-Asp-Tyr-Ala

◖ T7 tag (11a.a.): Met-Ala-Ser-Met-Thr-Gly-Gly-Gln-Gln-Met-Gly

Figure 2. (A) The hydropathy plot of ACAT2 according to Kyte and Doolittle. (B) The transmembrane regions of ACAT2, depicted as dark boxes as predicted by the PhD program (T1-T7) or by the TMpred program (T1-T8). (C) Diagram demonstrating sites of insertion to produce various epitope-tagged human *ACAT2* DNA constructs. For each construct, the number of the amino acid after which the HA tag was inserted is indicated in the parentheses. Each construct listed contained a T7 tag at the C termini. The peptide sequences of HA and T7 are given at the bottom.

against antigenic site(s) within a.a. 384–433 (DM94), but were unable to produce antibodies against any other region of hACAT2. To circumvent this problem, we inserted the HA tag (9 a.a.) into various hydrophilic regions flanking the two sides of each putative TMD. To ensure that the HA tag insertion does not cause orientation change in the C-terminal, we also inserted the T7 tag (11 amino acids) at the end of each construct. This insertion allowed us to monitor the sidedness of the C termini for each tagged proteins (Figure

2C). We used two algorithms, the PhD prediction (Rost *et al.,* 1995) and the TMpred prediction (Hofmann and Stoffel, 1993), for making TMD predictions (Figure 2B). The sites of insertion of the tags are shown in Figure 2C. The sequences of the HA tag and the T7 tag are shown at the bottom of Figure 2. The various epitope-tagged constructs were expressed by transient expressions in AC29 cells. Their expressions were monitored by Western blotting with the anti-hACAT2 antibodies DM56 as the primary antibodies, and by

A
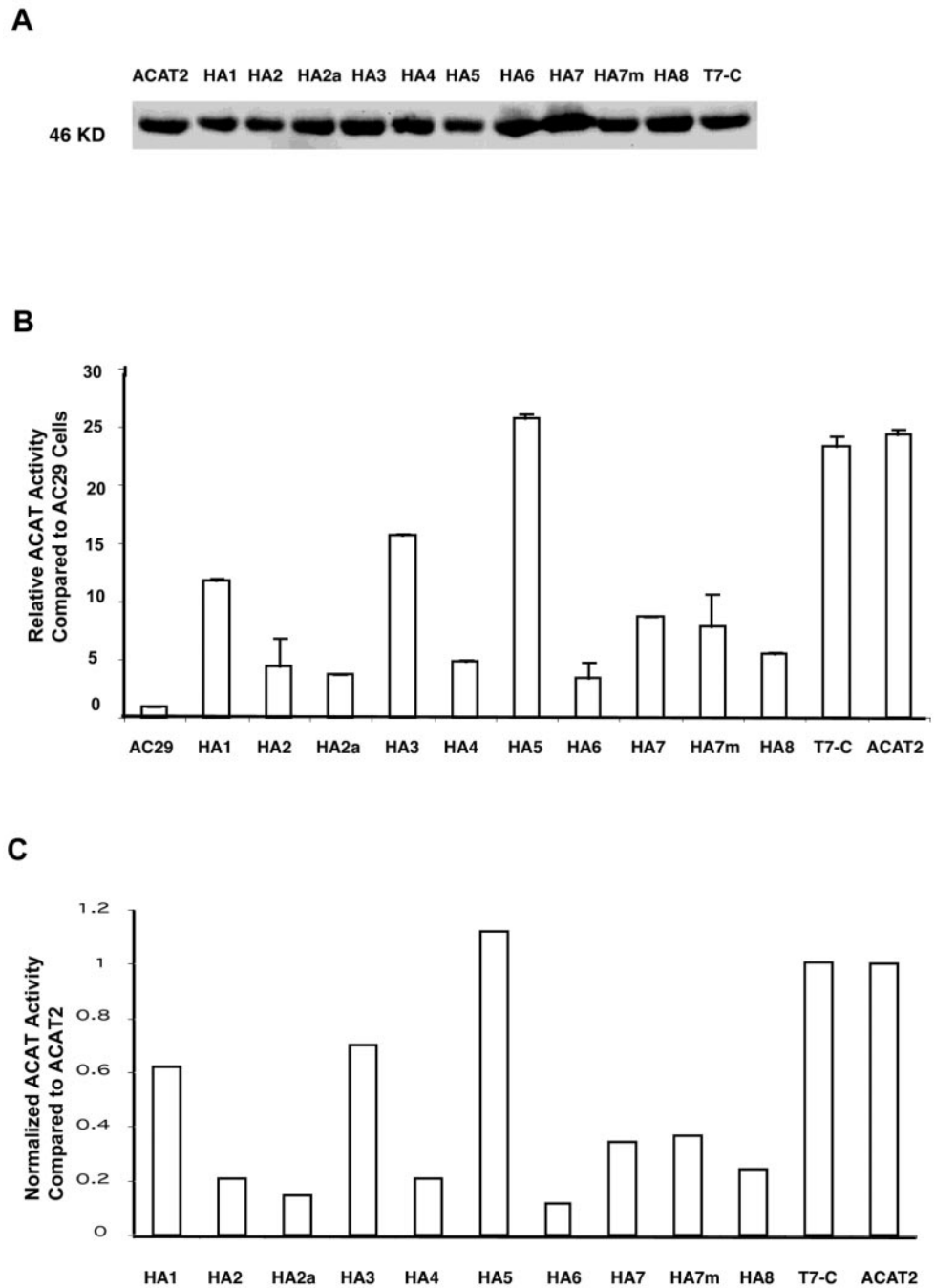
Figure 3. (A) Analyzing the expressions of various HA-tagged ACAT2s by Western blotting. AC29 cells were transiently transfected with individual HA-tagged *ACAT2* cDNA constructs as indicated. T7-C is abbreviation for the construct *ACAT2-T7* described in Figure 2A. The immunoblot was analyzed with the specific anti-ACAT2 antibodies DM56 according the method described in MATERIALS AND METHODS. The results were representative of two separate experiments. (B) Relative rates of cholesteryl ester biosynthesis in intact cells expressing various HA-tagged ACAT2 proteins as indicated. AC29 cells were transiently transfected with various indicated HA-tagged *ACAT-2* cDNA constructs, then pulsed with [³H]oleate for 2 h to measure the rate of cholesteryl ester biosynthesis in intact cells by the method described in MATERIALS AND METHODS. Enzyme activity assays were performed in duplicate. Values obtained for transfectant cells were expressed as relative activity compared with AC29 cells, by using the value obtained in mock-transfected AC29 cells as 1.0. Results shown were averages of two separate experiments; sizes of bars indicated one SE. (C) Normalized ACAT activity of various HA-tagged ACAT2s. These values were calculated by using the individual values reported in Figure 3B divided by the individual intensities of the corresponding ACAT2 bands shown in Figure 3A. Quantitations of ACAT2 bands were by densitometric analysis.

using ACAT activity assay in intact cells (Chang *et al.*, 1986). The results show that all the tagged or the untagged ACAT2 constructs were expressed as a single band with an apparent molecular mass of 46 kDa on SDS-PAGE (Figure 3A). Degradative fragment(s) from the full-length recombinant hACAT2s were not detectable (our unpublished data). For ACAT2s that carried the HA tag and/or the T7 tag, if the anti-HA antibodies and/or the T7 tag were used as the primary antibodies for Western analyses, the same results as shown in Figure 3A were obtained (our unpublished data). The ACAT activities of various tagged ACAT2 versus those of the untagged ACAT2 expressed in AC29 cells are shown in Figure 3B. Based on the protein expression data (Figure 3A) and the activity measurement data (Figure 3B), we calculated the normalized ACAT activity for each tagged ACAT2 relative to that of the untagged ACAT2. The results

(Figure 3C) show that 1) the insertion of the T7 tag at the C termini or the insertion of the HA tag at the HA5 site did not significantly alter ACAT activity; 2) the insertion of the HA tag at the HA1 or HA3 site caused a significant decrease in ACAT activity; the activity loss was ~30–40%; and 3) the insertion of the HA tag at HA2, HA2a, HA4, HA6, HA7, HA7m, or HA8 sites caused a major decrease in ACAT activity; the activity loss ranged from ~65 to 90%.

To determine the sidedness of the individual tag along the ER membrane, we performed cytoimmunofluorescence. The double immunostaining procedure was used by adding the DM56 antibodies and the anti-HA (or the anti-T7) antibodies simultaneously. The DM56 antibodies were viewed in red, whereas the anti-HA or the anti-T7 antibodies were viewed in green. The concentrations of the DM56 and the anti-HA antibodies (or the anti-T7 antibodies) were used such that the red color did not overlap significantly in the green filter, and vice versa. Additional control experiments showed that if the primary antibodies were deleted from the immunostaining procedure, no significant signal was seen when either the red or the green secondary antibodies was used alone (our unpublished data). The results of the experiments are summarized in Figure 4. Each photo is representative of 30 or more randomly chosen fields. The red color shown in columns 1 and 3 indicated that all of the tagged ACAT2s were located in the nuclear envelope and the entire reticulate network, demonstrating that they were mainly located in the ER membrane. For all of the tagged ACAT2 examined, the red color could be readily seen in either digitonin-treated cells (column 1) or in saponin-treated cells (column 3), indicating that the N-terminal segment of various recombinant ACAT2 remained to be located in the cytoplasmic side of the ER membrane. We next used the anti-T7 antibody (viewed in green) to examine the sidedness of the C termini of various recombinant ACAT2s, and found that the green color could also be seen in either digitonin-treated cells, or in saponin-treated cells. A representative photo, taken from ACAT2 tagged with T7 at the C termini, is shown in the bottom row of Figure 4. This result held true for all the constructs that contained an additional HA tag inserted at various regions (our unpublished data). Together, the data indicated that the C-terminal segment of ACAT2 with or without the additional HA sequence also resided in the cytoplasmic side of the ER membrane.

When the anti-HA antibodies were used and viewed (in green) for the ACAT2-HA1 protein, the green color could only be seen in saponin-treated cells, but not in digitonin-treated cells (Figure 4, row 1). In contrast, for the ACAT2-HA2 protein, the green color could be seen in saponin-treated cells as well as in digitonin-treated cells (Figure 4, row 2). For all other HA-tagged ACAT2 listed on the left-hand side of Figure 4 (i.e., ACAT2-HA2a-8), the green color could be readily seen in either digitonin-treated cells or in saponin-treated cells (Figure 4, columns 2 and 4).

Cytoimmunofluorescence of Various Mab1-tagged ACAT2

The results described above suggest that hACAT2 contains only two detectable TMDs. Based on the prediction algorithms described in Figure 2B, they are probably located between amino acids 124 and 144, and between 155 and 179. To test the two TMD model by using a different tag, we
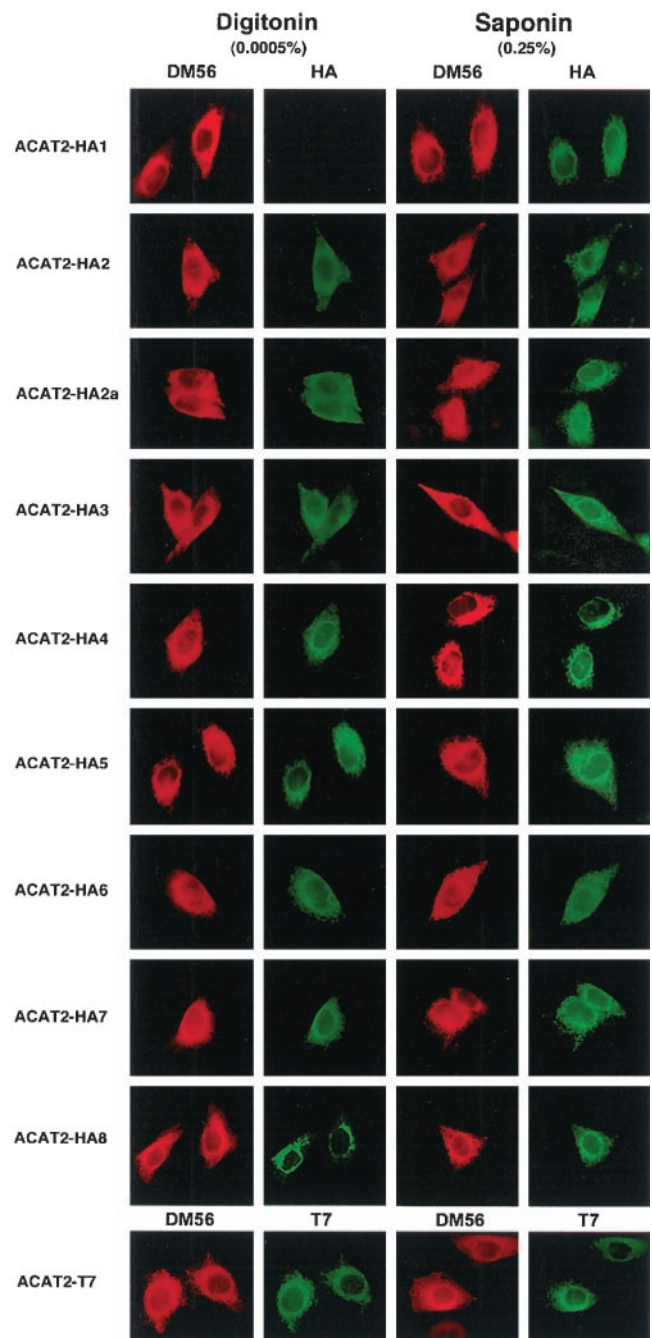
Figure 4. Determining the sidedness along the ER membranes of the HA tags in ACAT2 by indirect cytoimmunofluorescence. AC29 cells transiently transfected with various HA-tagged *ACAT2* constructs (indicated at the left) were doubly immunostained with the ACAT2 N-terminal specific antibodies DM56 providing the red color, and the anti-HA antibodies providing the green color. The left two columns show immunostainings after cells were permeabilized with digitonin; the right two columns show immunostainings after cells were permeabilized with saponin. In the last row, the double immunostainings were performed using DM56 providing the red color and the anti-T7 antibody providing the green color.
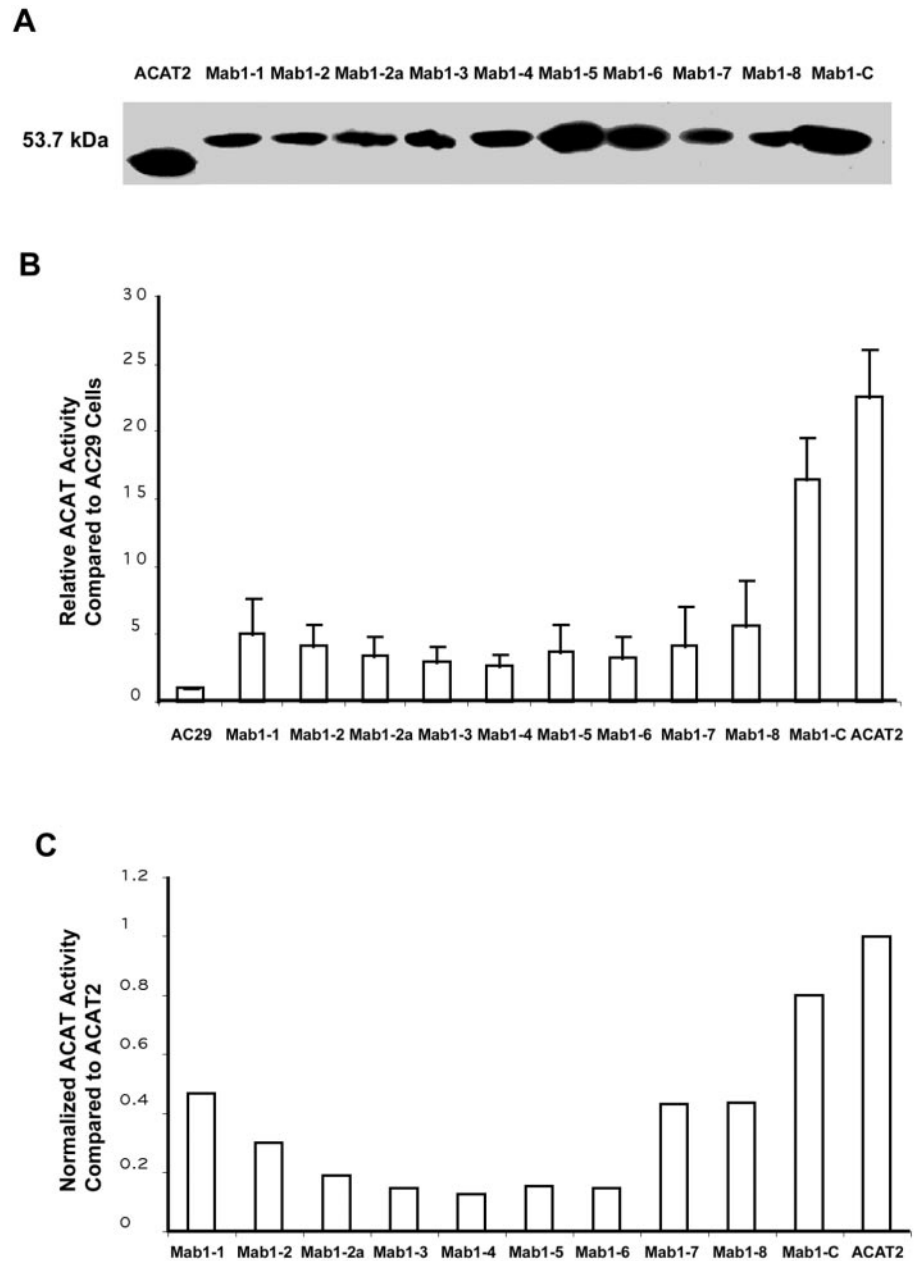
Figure 5. (A) Analyzing the expressions of various Mab1-tagged ACAT2s by Western blotting. (B) Relative rates of cholesteryl ester biosynthesis in intact cells expressing various Mab1-tagged ACAT2 proteins as indicated. C. Normalized ACAT activity of various Mab1-tagged ACAT2s. The experiments were performed and the results were presented in the same manner as described in Figure 3, A–C, but using various Mab1-tagged ACAT2 constructs (instead of the HA-tagged ACAT2 constructs). The sites of insertion for the Mab1 tag, indicated as Mab1 1-8, or as Mab1-C, were the same as the sites of insertion for the HA tag, indicated as HA 1-8 and shown in Figure 2C.

engineered a larger tag (64 amino acid), designated as the Mab1 tag, at various sites of ACAT2. The sequence of Mab1, MVGEEKMSLRNRLSKSRENPEEDEDQRNPAKESLETPSN-GRIDIKQLIAKKIKLTAEAEELKPF, is the same as the first 64 a.a. of hACAT1 (Chang *et al.*, 1993) and contains multiple lysines and arginines, and is therefore very sensitive to digestion by trypsin. In addition, this sequence is recognized by a specific mAb MACAT1 (Chang *et al.*, 1998). In cytoimmunofluorescence studies, the signal provided by the antibody MACAT1 is significantly stronger than that provided by the anti-HA antibodies (our unpublished data). The nomenclature and sites of insertion for the Mab1 tags corresponded exactly with those for the HA tags as indicated in Figure 2.

We expressed various Mab1-tagged ACAT2 constructs in AC29 cells by transient transfection and monitored their protein expressions and ACAT activities by the same procedures as described previously. The results show that all of the tagged ACAT2 were expressed as a single band with an apparent molecular mass of 53.7 kDa by SDS-PAGE (Figure 5A). Degradative fragment(s) from the full-length recombinant hACAT2s were not detectable (our unpublished data). We next compared the ACAT activities of various Mab1-tagged ACAT2 with that of the untagged ACAT2 (Figure

5B), and calculated the normalized ACAT activity for each tagged ACAT2 relative to that of the untagged ACAT2 (Figure 5C). The results show that the insertions of the Mab1 tag caused losses in ACAT activities to various extents. The tagged ACAT2s remained at least partially enzymatically active; with percentage of activity remaining ranging between 30 and 40% for tagged ACAT2s Mab1-1, Mab1-2, Mab1-7, and Mab1-8; and between 10 and 20% for tagged ACAT2s Mab1-2a, Mab1-3, Mab1-4, Mab1-5, and Mab1-6. The tagged ACAT Mab1-C remained 80% as active as the untagged ACAT2. We next performed double immunostaining experiments, by using the DM54 (which recognizes the same antigenic site as DM56 and stained the N-terminal of hACAT2, viewed in red) and the MACAT1 (viewed in green) simultaneously. The results are summarized in Figure 6. Each photo is representative of at least 30 randomly chosen fields. These results indicate that both the N-terminal and the Mab1 sites located at the C-terminal are accessible in digitonin-treated cells or in saponin-treated cells. The Mab1–1 site (inserted before 146th a.a.) is the only site that was accessible in saponin-treated cells but not in digitonin-treated cells. The Mab1-2 site (inserted before 195th a.a.) as well as all other Mab1-tagged ACAT2 listed on the left-hand side of Figure 6 are all accessible in either digitonin-treated cells or in saponin-treated cells (Figure 6, columns 2 and 4). These results corroborated the data by using the HA tag insertion method and show that the same two TMDs have been detected.

Protease Protection Assay of Various Mab1-tagged ACAT2 in Membrane Vesicles

We next tested the two TMD model by using the protease protection assay. This method is based on the premise that if the membrane vesicles that contain ACAT2 remain sealed, only the ACAT2 peptide segments located in the cytoplasmic side of the membrane are susceptible to trypsin digestion. We expressed various Mab1-tagged ACAT2 proteins and then prepared sealed membranes from homogenates of transfected cells, treated the membranes with or without the detergent Triton X-100, and performed protease digestions by using increasing amounts of trypsin. To serve as control, we monitored the lumenal ER protein marker BiP by using Western blotting and showed that BiP was partially protected by membranes against trypsin digestion, but only if the membranes were not treated with Triton X-100 (Figure 7A, bottom row). This result validated the use of the protease protection assay in our system. We next monitored the various Mab1-tagged ACAT2s. The results (summarized in Figure 7A) showed that only the Mab1-1 site, but not any other Mab1 sites tested, could be partially membrane-protected against trypsin digestion, implying that only the Mab1-1 site of ACAT2 is located in the lumenal side of the membranes.

As shown in the last lane of Figure 7A, the lumenal ER protein BiP was partially susceptible to trypsin digestion in the absence of Triton X-100, suggesting that the microsomal vesicles isolated in vitro became leaky during trypsin digestion. Regarding the membrane protection against trypsin digestion, a more reliable procedure was developed by Macri and Adeli (1997, who showed that in monolayers of intact cells permeabilized with digitonin, the lumenal proteins residing in the ER membranes remained largely intact
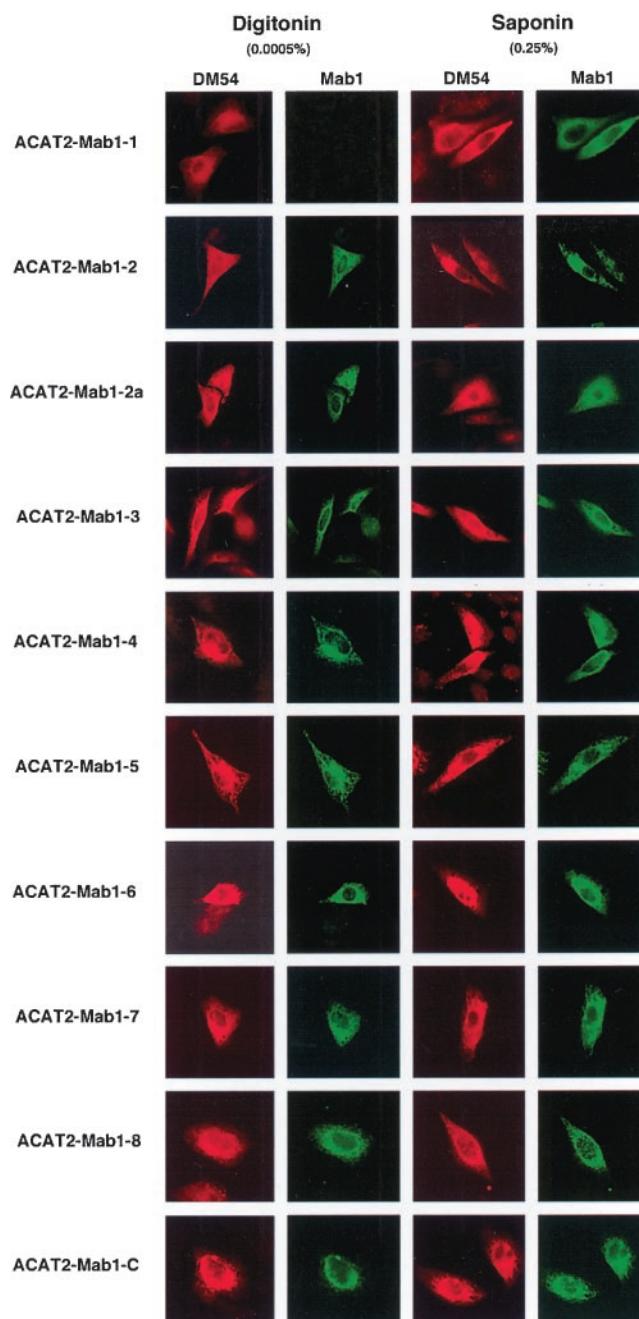
Figure 6. Determining the sidedness along the ER membranes of the Mab1 tags in ACAT2 by indirect cytoimmunofluorescence. The experiments were performed and the results were presented in the same manner as described in Figure 4, but using various Mab1-tagged ACAT2 constructs as indicated. The ACAT2 N-terminal specific antibodies DM54 were used and viewed in red, and the mAb against Mab1 was used and viewed in green.

during trypsin digestion. We adopted this procedure and repeated the trypsin digestion experiment, after transfected cells were permeabilized with either digitonin (at 0.002%) or with saponin (at 0.025%). The control experiment (last lane
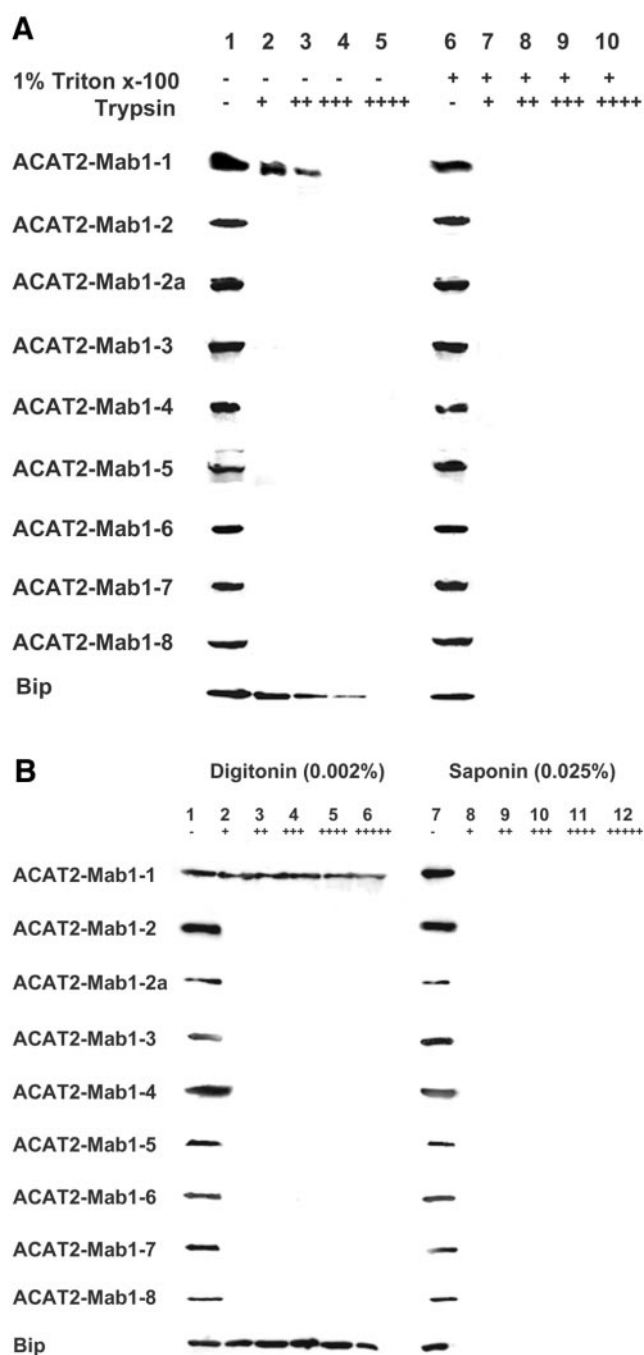
Figure 7. Trypsin protection assay. (A) Microsomes prepared from AC29 cells transiently transfected with various Mab1-tagged ACAT2 constructs as indicated were processed for trypsin protection assay, by using method 1 described in MATERIALS AND METHODS. Each membrane preparation was treated with or without Triton X-100 as indicated, and then treated without or with increasing amounts of trypsin as indicated. The final concentration of trypsin (in units per milliliter) present in each sample was as follows: 0 (−), 0.25 (+), 0.5 (++), 1.25 (+++), or 2.5 (++++). (B) Monolayers of AC29 cells transiently transfected with various Mab1-tagged ACAT2 constructs were permeabilized with digitonin or with saponin as indicated and were processed for trypsin pro-

of Figure 7B) showed that, when cells were permeabilized with the cholesterol binder digitonin at low concentration, the lumenal ER protein BiP was resistant to trypsin, indicating that under this condition, the ER membrane remained sealed during trypsin digestion. Instead, when cells were permeabilized with saponin (a purified form of digitonin) at higher concentration, BiP became very susceptible to trypsin, indicating that under the latter condition, ER membrane becomes leaky, allowing trypsin to gain access to the ER interior. Additional results of Figure 7B showed that in digitonin-treated cells, only the Mab1 tag located in site 1 was protected against trypsin digestion. In saponin-treated cells, all of the Mab1 tags were susceptible to trypsin. Thus, using two different procedures, the protease protection data fully corroborated the cytoimmunofluorescence data described above. These results suggest that within ACAT2 there are only two detectable TMDs.

Location of the Putative ACAT Active Site along the ER Membrane

We next sought to identify certain key residue(s) involved in ACAT catalysis and determine its location along the ER membrane. A conserved serine (S245 in hACAT2) and a conserved histidine (H434 in hACAT2) have been implicated as candidate active site residues. To test the functionality of S245 and H434, we created four point mutants (A2-H434A, A2-H434N, A2-S245A, and A2-S245L) by site-specific mutagenesis, and then expressed these mutants individually in AC29 cells by transient transfections. The enzyme activities of these mutants, along with that of the wild-type ACAT2, were measured in intact cells (Figure 8A), and normalized by their relative ACAT2 protein expression levels (Figure 8B). The results (Figure 8C) show that the A2-S245A mutant and the A2-S245L mutant still contained a significant amount of residual enzyme activity, whereas the A2-H434A mutant and the A2-H434N mutant contained essentially a negligible amount of enzyme activity.

H434 is located within a long hydrophobic peptide segment of >20 a.a. (Hofmann, 2000). For human ACAT2, this "signature sequence" corresponds to a.a.420–442. To determine the location of the peptide that precedes H434, we created a GST fusion protein, with GST fused at the N terminus of a peptide comprised of two repeats of the ACAT2 peptide$_{a.a.\ 384-433}$ (sequence shown in Figure 9A). This fusion protein was expressed in *Escherichia coli*, purified to homogeneity, and was used to produce rabbit polyclonal antibodies DM94. The affinity-purified DM94 specifically recognizes human HisACAT2 expressed in CHO cells as a single 51-kDa protein, as shown by Western analysis (Figure

Figure 7 (cont). tection assay by using method 2 described in MATERIALS AND METHODS. The final concentration of trypsin (in units per milliliter) present in each sample was as follows: 0 (−), 18.6 (+), 37.1 (++), 74.3 (+++), 148.5 (++++), or 297.0 (+++++). For Figure 7, A and B, Western blotting using the DM10 polyclonal antibodies monitored the presence of the MAB1 tag in the recombinant ACAT2 proteins (53.7 kDa). Western blotting using the anti-GRP78 monoclonal antibodies (Transduction Laboratories, Lexington, KY) monitored the presence of the ER protein BiP (78 kDa) in the ER lumen, as shown in the last lane. The data shown are representative of three separate experiments.
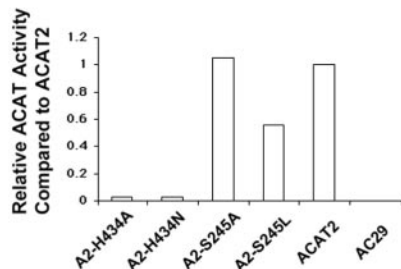
A. Cholesteryl Ester Biosynthesis in Intact Cells
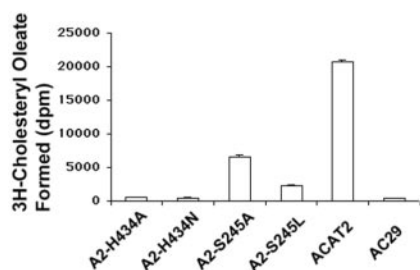
B. Immunoblot with DM54
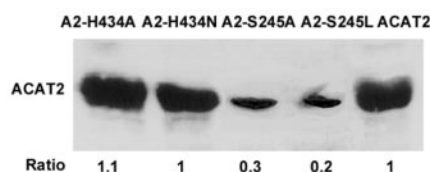
C. Normalized Relative ACAT Activity

Figure 8. Enzyme activities of ACAT2 mutants A2-H434A, A2-H434N, A2-S245A, and A2-S245L. (A) Cholesteryl ester biosynthesis in intact cells. (B) Immunoblot analysis using anti-ACAT2 antibodies DM54. (C) Normalized ACAT activity of the ACAT2 mutants. The experiments were conducted and calculated in the same manner as described in Figure 3. Enzyme activity assays were performed in duplicate. Results shown are representative of two separate experiments.

9B). To determine the sidedness of peptide$_{a.a. 384-433}$ of hACAT2 in the ER, we performed double cytoimmunofluorescence experiments by adding the DM94 antibodies and the anti-histidine tag mAb (HisMab) simultaneously to cells that express HisT7-hACAT2. HisT7-ACAT2 contains a 6 × histidine sequence and the T7 sequence as its N terminus. Mock-transfected AC29 cells were used as a negative control. The result shows that, in AC29 cells, the HisTag antibody nonspecifically stains the nuclei (Figure 9C, bottom). In cells expressing HisT7-hACAT2, both the HisTag antibody and the DM94 gave characteristic ER staining pattern (Figure 9C, top). The signals were essentially identical whether the cells were permeabilized with digitonin or with saponin. This result corroborates the result obtained by using the ACAT2-HA6 (Figure 4), and demonstrates that the antigen-

ic/hydrophilic region of the peptide$_{a.a. 384-433}$ resides at the cytoplasmic side of the ER.

To further probe the environment near the putative active site H434, we produced a specific HA-tagged ACAT2 construct, designated as ACAT2-HA7m, by inserting the HA tag before a.a. 432, (which is two residues before H434). We expressed this construct in AC29 cells by transient transfections. Activity measurement showed that mutant ACAT2-HA7m contained ~35% of the activity found in wild-type ACAT2 (Figure 3C, lane 9). We then performed the immunoblot analysis and the cytoimmunofluorescence analysis. The results show that in immunoblot analysis, the HA tag present in ACAT2-HA7m could be detected (Figure 10B; lane 2). In contrast, in cytoimmunofluorescence analysis, irrespective of whether the cells were exposed to the mild detergent (0.0005% digitonin) or to the stronger detergent (0.25% saponin), we have consistently failed to detect the HA signal (Figure 10A; lanes 2 and 4). The control experiment shows that the N-terminal region of ACAT2-7m could be detected in immunoblot (by DM54; Figure 10B, lane 2), and by cytoimmunofluorescence (by DM56; Figure 10A, lanes 1 and 3).

DISCUSSION

The ACAT Active Site, the Proposed ACAT2 Membrane Topology, and the Location of the Active Histidine

Our current work shows that a conserved histidine (H434 in hACAT2) may be essential for ACAT catalysis, whereas a conserved serine (S245 in hACAT2) is not. In results presented as an abstract, we have tested the functionality of the conserved serine (S269) and histidine (H460) in hACAT1, and obtained the same results (Lu *et al.*, 2002a). The results of the cytoimmunofluorescence assay (Figures 4 and 6) and the results of the protease protection assay (Figure 7, A and B) indicate that ACAT2 contains only two detectable TMDs, located near the N-terminal region. The existence of these two TMDs has been predicted by the PhD algorithm and the TMpred algorithm. In contrast, other potential TMDs predicted by the PhD algorithm or the TMpred algorithm (Figure 2B) cannot be detected under our assay conditions. The methods used by us cannot directly detect/view the membrane imbedded region(s). Thus, our current results cannot rule out the possibility that one or more hydrophobic regions, predicted as potential TMD by various algorithms, may be partially or entirely embedded in one leaflet of the lipid bilayer. This type of arrangement has been demonstrated at the crystal structure level for the membrane bound enzyme prostaglandin H$_2$ synthase-1 (Picot *et al.*, 1994) and for a glycerol-conducting channel (Fu *et al.*, 2000). The results presented in Figure 10 show that the hydrophobic peptide comprising the putative active H434 is in a shielded state such that the HA tag inserted nearby is prevented from reacting with the HA antibodies. This observation led us to speculate that H434 may be located within the plane of the membrane lipid bilayer. Similar to this finding, as part of our work on hACAT1 topology studies, we had produced a mutant hACAT1-HA7m, by inserting the HA tag before a.a.459, which is one a.a. before the putative active H460. We found that the HA tag in hACAT1-HA7m could not be detected by either cytoimmunofluorescence analysis or by

A. Antigenic Site for Antibodies DM94 (ACAT2 a.a 384-433)
STSFSNYYRTWNVVVHDWLYSYVYQDGLRLLGARARGVAMLGVFLVSAVA

Figure 9. (A) Peptide sequence of human ACAT2$_{a.a.\ 384-433}$ used to raise rabbit polyclonal antibodies DM94. (B) Specificity of antibodies DM94 against human ACAT2 analyzed by Western blot analysis. The immunoblot was performed as described in MATERIALS AND METHODS. (C) Sidedness of the peptide a.a.384–433 as probed by indirect cytoimmunofluorescence. The experiments were performed according to the method described in Figure 4, with the DM94 antibodies providing the green color and the antimonoclonal antibody HisTag providing the red color. The affinity purified DM94 was used at 5 μg/ml. The histidine mAb HisTag (Novagen, Madison, WI) was used after a 1:1000 dilution from a 0.2 mg/ml stock.

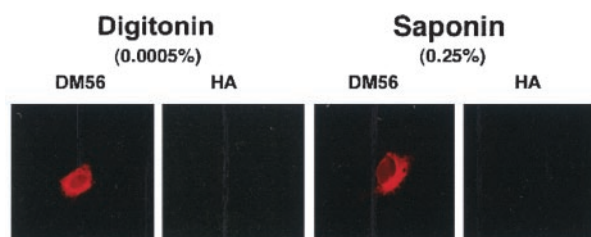## B. Immunoblot
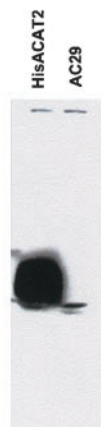
C. Immunofluorescence
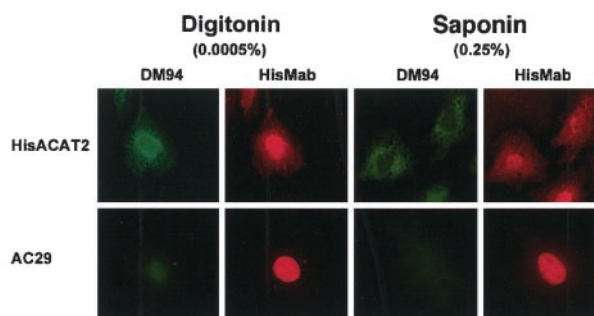
immunoblot analysis (results described on p. 23,283 of Lin *et al.*, 1999). Thus, despite the significant difference in their membrane topology, the conserved hydrophobic peptide segment that comprises the putative active histidine in ACAT1 and ACAT2 may both be partially imbedded within the lipid bilayer. This arrangement may allow both ACAT1 and ACAT2 to produce cholesteryl esters within the lipid bilayer and serve their dual roles: to produce cholesteryl esters that can move to the cytoplasm as lipid droplets and/or move to the lumen of internal membranes and participate in the lipoprotein assembly processes (discussed in Chang *et al.*, 2001b). To put these considerations together, we propose a working model for ACAT membrane topology, shown in Figure 11.

The Discrepancy between Our Current Result and That of Joyce and Colleagues (Joyce et al., 2000)

Previously, Joyce and colleagues tested the effects of replacing the conserved serine with leucine in ACAT1 and ACAT2, and concluded that the conserved serine may be essential for ACAT catalysis. These investigators expressed their mutant constructs and measured the enzyme activities in manners similar to ours; however, they did not perform immunoblot analysis to normalize the difference in the protein expression levels. As shown in our current work, the S245L mutation caused the mutant ACAT2 protein to be expressed at much a lower level than the wild-type ACAT2 (Figure 8). Thus, although the conserved serine may be important for ACAT protein stability, it is not essential for ACAT catalysis.

Joyce and colleagues also reported that both monkey ACAT1 and monkey ACAT2 contained five TMDs (Joyce *et al.*, 2000). A key difference between our study and their study is that we relied mainly on the tag insertion approach, whereas Joyce and colleagues relied mainly on the trunca-

A. Cytoimmunofluorescence of ACAT2-HA7m

B. Immunoblot with Anti-HA Antibody
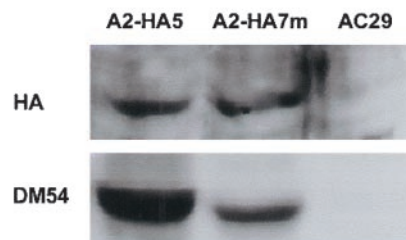
Figure 10. Detecting the HA tag inserted before a.a.432 of ACAT2 by cytoimmunofluorescence or by immunoblot. AC29 cells were transfected with the construct ACAT2-HA7m, with the HA tag inserted before a.a.432. (A) Indirect cytoimmunofluorescence of transfected cells. The experiments were conducted in the same manner as described in Figure 4. (B) Immunoblot of transfected cell lysates. Lysates of AC29 cells and cells that express ACAT2-HA5 (abbreviated as A2-HA5) were used as the negative and positive controls. The experiments were conducted in the same manner as described in Figure 3. Results shown are representative of two separate experiments.
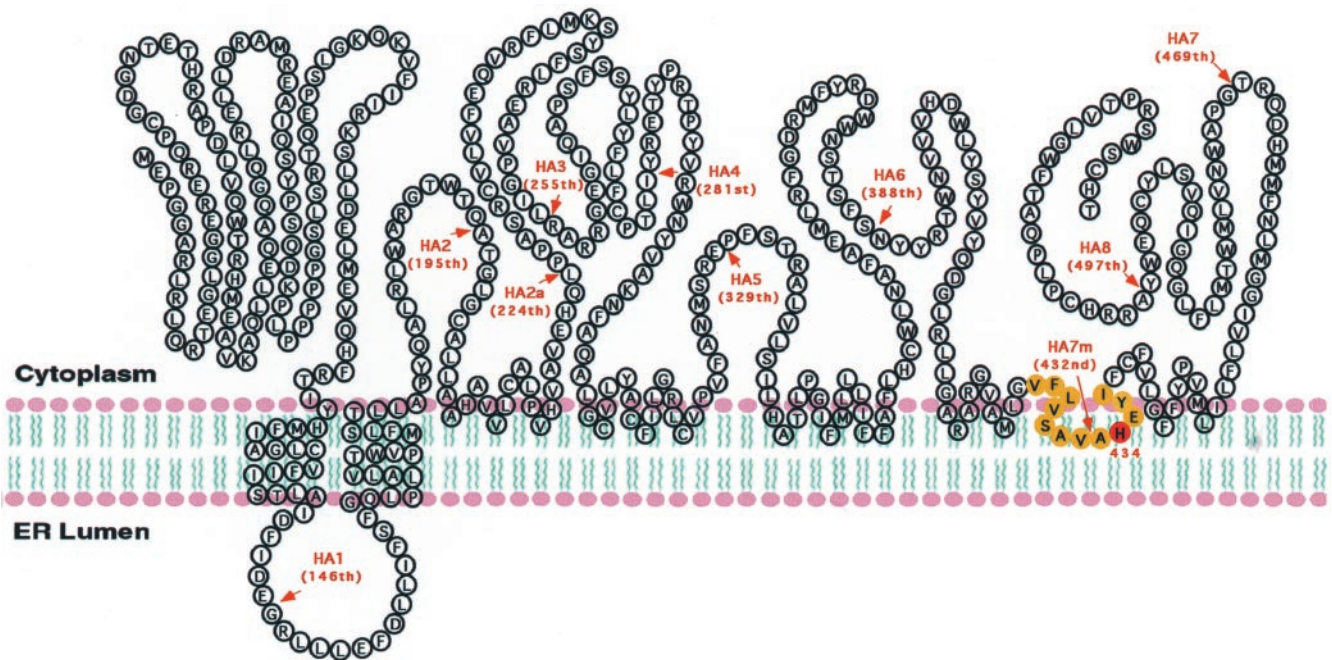
Figure 11. The proposed membrane topology of hACAT2 expressed in CHO cells. The arrows indicated the positions where the HA tags were inserted. This model proposes that ACAT2 may only contain two detectable TMDs and that the hydrophobic peptide segment peptide (indicated in yellow color) containing the putative active histidine (H434) may be partially imbedded within the cytoplasmic side of the lipid bilayer. The extent of insertion of the hydrophobic peptide into the lipid bilayer is unknown. The model is drawn to suggest that additional hydrophobic region(s) may also be partially imbedded within the lipid bilayer (see text).

tion approach. They prepared a series of the target proteins successively truncated from the C termini after each of the predicted TMDs; the topology was then determined by monitoring the membrane sidedness of a tag at the C termini of each fusion protein. These investigators did not report the percentage of ACAT activity remaining in any of the truncated proteins. We show in our current study that each tagged ACAT2 is at least partially enzymatically active; we also show that the C termini of all of these tagged ACAT2 reside in the cytoplasmic side of the ER (Figure 4). Thus, inserting the HA tag at various flanking sites did not cause orientation change at the ACAT2 C-terminal. In our unpublished results, we had prepared various hACAT1 constructs by using the insertion approach and the truncation approach. Our results showed that using the insertion approach, the various tagged proteins retained at least partial enzyme activity, whereas the various truncated proteins had completely lost their enzyme activities. In principle, both the insertion approach and the truncation approach run the risk of altering the membrane topology of the target protein. To resolve the discrepancy between our results and the results of Joyce and colleagues, other methods for membrane topology determinations that produce minimal structural perturbations of ACAT will be needed.

Regarding the ACAT2 topology, one more major discrepancy existed between our current result and the result of Joyce and colleagues: our results show that the C termini is in the cytoplasmic side of the ER, whereas Joyce and colleagues showed that the C termini was in the lumen of the ER. The exact cause of the discrepancy is not known at

present. Below, we offer a certain clue: to determine the sidedness of the C terminus, both groups used the full-length ACAT2, and placed certain tags near or at its C termini. Both groups used AC29 cells as the host for expressing the tagged constructs and used cytoimmunofluorescence to examine the sidedness of the tag after detergent permeabilization of cells. We used the double immunostaining procedure for cytoimmunofluorescence and made sure that the two signals colocalized when viewed under confocal microscopy. Joyce and colleagues did not use the double immunostaining procedure for their studies. It has been our experience that the transfection procedure (used by both groups) tends to produce some sick and/or dying cells; these cells can be as many as 5% of the total cell population. These cells may not be true transfectants but they tend to adsorb antibodies nonspecifically. The use of these cells for data collection should be avoided. The use of double immunofluorescence ensured that the investigators were viewing the desirable gene product expressed in the transfected cells.

The Difference between ACAT1 and ACAT2 in Terms of Membrane Topology

The hydropathy plots (Figure 2A; Lin *et al.*, 1999) of ACAT1 and ACAT2 are very similar, though not the same. Although the seven-TMD model for ACAT1 described previously (Lin *et al.*, 1999) is very close to prediction by various algorithms, the two-TMD model for ACAT2 is strikingly different from prediction. According to the current knowledge (described in textbooks (Alberts *et al.*, 1994; Lodish *et al.*, 1999), to form

multispanning TM proteins in the ER, multiple topogenic sequences (i.e., multiple uncleaved signal anchoring sequences and/or stop-transfer sequences) are needed. These sequences interact with the ER transmembrane protein channel machinery in a reversible manner. The topogenic sequences are hydrophobic peptides capable of forming α-helices. Additional features that determine the functions of the topogenic sequences are possible but have not been generalized. Sequence comparisons show that although several highly conserved peptide sequences can be identified in ACAT1 and ACAT2, most of the TMDs of ACAT1 do not share high sequence homology with the corresponding domains present in ACAT2. It seems possible that the differences in the putative TMD sequences may be the underlying cause for the difference in membrane topology of ACAT1 and ACAT2. It is also possible that similar to ACAT1, multiple topogenic sequences are present in ACAT2. However, their membrane insertion/stop transfer functions may be masked by interaction(s) with other sequence(s) within the ACAT2 protein, or with nonbilayer lipid, or with other protein(s).

ACKNOWLEDGMENTS

REFERENCES

Alberts, B., Bray, D., Lewis, J., Raff, M., Roberts, K., and Watson, J.D. (1994). Molecular Biology of the Cell, New York: Garland Publishing.

Anderson, R.A., Joyce, C., Davis, M., Reagan, J.W., Clark, M., Shelness, G.S., and Rudel, L.L. (1998). Identification of a form of acyl-CoA:cholesterol acyltransferase specific to liver and intestine in nonhuman primates. J. Biol. Chem. 273, 26747–26754.

Buhman, K.F., Accad, M., and Farese, R.V., Jr. (2000a). Mammalian acyl-CoA:cholesterol acyltransferases. Biochim. Biophys. Acta 1529, 142–154.

Buhman, K.K., Accad, M., Novak, S., Choi, R.S., Wong, J.S., Hamilton, R.L., Turley, S., and Farese, R.V., Jr. (2000b). Resistance to diet-induced hypercholesterolemia and gallstone formation in ACAT2-deficient mice. Nat. Med. 6, 1341–1347.

Buhman, K.K., Chen, H.C., and Farese, R.V., Jr. (2001). The enzymes of neutral lipid synthesis. J. Biol. Chem. 276, 40369–40372.

Cadigan, K.M., Heider, J.G., and Chang, T.Y. (1988). Isolation and characterization of Chinese hamster ovary cell mutants deficient in acyl-coenzyme A:cholesterol acyltransferase activity. J. Biol. Chem. 263, 274–282.

Cao, G., Goldstein, J.L., and Brown, M.S. (1996). Complementation of mutation in acyl-CoA:cholesterol acyltransferase (ACAT) fails to restore sterol regulation in ACAT-defective sterol-resistant hamster cells. J. Biol. Chem. 271, 14642–14648.

Cases, S., et al. (1998a). ACAT-2, a second mammalian acyl-CoA: cholesterol acyltransferase. Its cloning, expression, and characterization. J. Biol. Chem. 273, 26755–26764.

Cases, S., et al. (1998b). Identification of a gene encoding an acyl CoA:diacylglycerol acyltransferase, a key enzyme in triacylglycerol synthesis. Proc. Natl. Acad. Sci. USA 95, 13018–13023.

Chang, C.C.Y., et al. (2000). Immunological quantitation and localization of ACAT-1 and ACAT-2 in human liver and small intestines. J. Biol. Chem. 275, 28083–28092.

Chang, T.Y., Chang, C.C.Y., and Cheng, D. (1997). Acyl-coenzyme A:cholesterol acyltransferase. Annu. Rev. Biochem. 66, 613–638.

Chang, T.Y., Chang, C.C.Y., Lin, S., Yu, C., Li, B.L., and Miyazaki, A. (2001a). Roles of acyl-coenzyme A:cholesterol acyltransferase-1 and -2. Curr. Opin. Lipidol. 12, 289–296.

Chang, T.Y., Chang, C.C.Y., Lu, X.H., and Lin, S. (2001b). ACAT catalysis may be completed within the plane of the membrane: a working hypothesis. J. Lipid Res. 42, 1933–1938.

Chang, C.C.Y., Chen, J., Thomas, M.A., Cheng, D., Del Priore, V.A., Newton, R.S., Pape, M.E., and Chang, T.Y. (1995). Regulation and immunolocalization of acyl-coenzyme A:cholesterol acyltransferase in mammalian cells as studied with specific antibodies. J. Biol. Chem. 270, 29532–29540.

Chang, C.C.Y., Doolittle, G.M., and Chang, T.Y. (1986). Cycloheximide sensitivity in regulation of acyl coenzyme A:cholesterol acyltransferase activity in Chinese hamster ovary cells. I. Effect of exogenous sterols. Biochemistry 25, 1693–1699.

Chang, C.C.Y., Huh, H.Y., Cadigan, K.M., and Chang, T.Y. (1993). Molecular cloning and functional expression of human acyl-coenzyme A:cholesterol acyltransferase cDNA in mutant Chinese hamster ovary cells. J. Biol. Chem. 268, 20747–20755.

Chang, C.C.Y., Lee, C.Y.G., Chang, E.T., Cruz, J.C., Levesque, M.C., and Chang, T.Y. (1998). Recombinant human acyl-CoA:cholesterol acyltransferase-1 (ACAT-1) purified to essential homogeneity utilizes cholesterol in mixed micelles or vesicles in a highly cooperative manner. J. Biol. Chem. 273, 35132–35141.

Fu, D., Libson, A., Miercke, L.J., Weitzman, C., Nollert, P., Krucinski, J., and Stroud, R.M. (2000). Structure of a glycerol-conducting channel and the basis for its selectivity. Science 290, 481–486.

Guo, Z., Cromley, D., Billheimer, J.T., and Sturley, S.L. (2001). Identification of potential binding sites in yeast and human acyl-CoA sterol acyltransferases by mutagenesis of conserved sequences. J. Lipid Res. 42, 1282–1291.

Hofmann, K. (2000). A superfamily of membrane-bound O-acyltransferases with implications for Wnt signaling. Trends Biochem. Sci. 25, 111–112.

Hofmann, K., and Stoffel, W. (1993). Tmbase: a database of membrane spanning proteins segments. Biol. Chem. Hoppe-Seyler 347, 166

Joyce, C.W., Shelness, G.S., Davis, M.A., Lee, R.G., Skinner, K., Anderson, R.A., and Rudel, L.L. (2000). ACAT1 and ACAT2 membrane topology segregates a serine residue essential for activity to opposite sides of the endoplasmic reticulum membrane. Mol. Biol. Cell 11, 3675–3687.

Kolodziej, P.A., and Young, R.A. (1991). Epitope tagging and protein surveillance. Methods Enzymol. 194, 509–519.

Lee, O., Chang, C.C.Y., Lee, W., and Chang, T.Y. (1998). Immunodepletion experiments suggest that acyl-coenzyme A:cholesterol acyltransferase-1(ACAT-1) protein plays a major catalytic role in adult human liver, adrenal gland, macrophages, and kidney, but not in intestines. J. Lipid Res. 39, 1722–1727.

Lee, R.G., Willingham, M.C., Davis, M.A., Skinner, K.A., and Rudel, L.L. (2000). Differential expression of ACAT1 and ACAT2 among cells within liver, intestine, kidney, and adrenal of nonhuman primates. J. Lipid Res. 41, 1991–2001.

Lin, S., Cheng, D., Liu, M.S., Chen, J., and Chang, T.Y. (1999). Human acyl-CoA:cholesterol acyltransferase-1 in the endoplasmic reticulum contains seven transmembrane domains. J. Biol. Chem. 274, 23276–23285.

Lodish, H., Berk, A., Zipursky, S.L., Matsudaira, P., Baltimore, D., and Darnell, J. (1999). Molecular Cell Biology, 4th ed. Scientific American Books. New York, NY: W. H. Freeman and Co.

Lu, X., Lin, S., Chang, C. C. Y. and Chang, T. Y. (2002a). Mutagenesis studies on ACAT1 reveal several residues, but not S269, that may be essential for ACAT catalysis (Abstract). The 3rd AHA National Conference on Atherosclerosis, Thrombosis, and Vascular Biology, Salt Lake City, UT.

Lu, X., Lin, S., Chang, C.C.Y., and Chang, T.Y. (2002b). Mutant acyl-coenzyme A:cholesterol acyltransferase 1 (ACAT1) devoid of cysteine residues remains catalytically active. J. Biol. Chem. *276*, 711–718.

Macri, J., and Adeli, K. (1997). Studies on intracellular translocation of apolipoprotein B in a permeabilized HepG2 system. J. Biol. Chem. *272*, 7328–7337.

Meiner, V.L., *et al.* (1996). Disruption of the acyl-CoA:cholesterol acyltransferase gene in mice: evidence suggesting multiple cholesterol esterification enzymes in mammals. Proc. Natl. Acad. Sci. USA *93*, 14041–14046.

Meiner, V.L., Tam, C., Gunn, M.D., Dong, L.M., Weisgraber, K.H., Novak, S., Myers, H.M., Erickson, S.K., and Farese, R.V., Jr. (1997). Tissue expression studies of mouse acyl CoA:cholesterol acyltransferase gene (Acact): findings supporting the existence of multiple cholesterol esterification enzymes in mice. J. Lipid Res. *38*, 1928–1933.

Oelkers, P., Behari, A., Cromley, D., Billheimer, J.T., and Sturley, S.L. (1998). Characterization of two human genes encoding acyl coenzyme A:cholesterol acyltransferase-related enzymes. J. Biol. Chem. *273*, 26765–26771.

Otto, J.C., and Smith, W.L. (1994). The orientation of prostaglandin endoperoxide synthases-1 and -2 in the endoplasmic reticulum. J. Biol. Chem. *269*, 19868–19875.

Picot, D., Loll, P.J., and Garavito, R.M. (1994). The X-ray crystal structure of the membrane protein prostaglandin H2 synthase-1. Nature *367*, 243–249.

Rost, B., Casadio, R., Fariselli, P., and Sander, C. (1995). Prediction of helical transmembrane segments at 95% accuracy. Protein Sci. *4*, 521–533.

Rudel, L., Lee, R., and Cockman, T. (2001). Structure, function, and regulation of ACAT. Curr. Opin. Lipidol. *12*, 121–127.

Sakashita, N., Miyazaki, A., Takeya, M., Horiuchi, S., Chang, C.C.Y., Chang, T.Y., and Takahashi, K. (2000). Localization of human acyl-coenzyme A:cholesterol acyltransferase-1 in macrophages and in various tissues. Am. J. Pathol. *156*, 227–236.

Spady, D.K., Willard, M.N., and Meidell, R.S. (2000). Role of acyl-coenzyme A:cholesterol acyltransferase-1 in the control of hepatic very low density lipoprotein secretion and low density lipoprotein receptor expression in the mouse and hamster. J. Biol. Chem. *275*, 27005–27012.

Yagyu, H., *et al.* (2000). Absence of ACAT-1 attenuates atherosclerosis but causes dry eye and cutaneous xanthomatosis in mice with congenital hyperlipidemia. J. Biol. Chem. *275*, 21324–21330.

Yu, C., Chen, J., Lin, S., Liu, J., Chang, C.C.Y., and Chang, T.Y. (1999). Human acyl-CoA:cholesterol acyltransferase-1 is a homotetrameric enzyme in intact cells and in Vitro. J. Biol. Chem. *274*, 36139–36145.

Yu, C., Zhang, Y., Lu, X., Chen, J., Chang, C.C.Y., and Chang, T.Y. (2002). The role of the N-terminal hydrophilic domain of acyl coenzyme A:cholesterol acyltransferase 1 on the enzyme's quaternary structure and catalytic efficiency. Biochemistry *41*, 3762–3769.